Asian Journal of Chemistry; Vol. 33, No. 1 (2021), 31-36

ASIAN JOURNAL OF CHEMISTRY

https://doi.org/10.14233/ajchem.2021.22908

Investigation of Organic Field-Effect Transistor (OFET) based NO_2 Sensing Response using Low-Cost Green Synthesized Zinc Oxide Nanoparticles

G. BALANAGIREDDY[1], ASHWATH NARAYANA[2] and M. ROOPA[3,*]

[1]Department of Electronics & Communication Engineering, Rajiv Gandhi University of Knowledge Technologies, IIIT Ongole Campus, Ongole-516330, India
[2]Department of Bio-Medical Engineering, Rajiv Gandhi Institute of Technology, R.T. Nagar P.O., Hebbal, Bengaluru-560032, India
[3]Department of Electronics & Communication Engineering, Dayanand Sagar College of Engineering, Bengaluru-560078, India

*Corresponding author: E-mail: surajroopa@gmail.com

Received: 21 July 2020; *Accepted*: 29 August 2020; *Published online*: 10 December 2020; AJC-20172

A low-cost and green-synthesized zinc oxide nanostructured particles are extensively studied owing to their remarkable and ample characteristics with less toxicity and eco-friendly approach. The present work comprehends the green synthesis of ZnO nanostructured particles using bougainvillea leaf extract-arbitrated microwave-assisted synthesis and their use in field effect transistor for nitrogen dioxide sensing at room temperature. The as-synthesized nanoparticles were characterized using analytical techniques; XRD determined the pure crystallite structure with no impurities, SEM confirmed the spherical shape of nanoparticles with ~20 nm (average particle size) and the atomic weight percentage were analyzed using EDAX, notable photophysical properties were revealed from absorption and emission spectra performed using UV-visible spectroscopy. Poly(3-hexylthiophene) and ZnO nanoparticles were employed in the field effect transistor (p-type) for NO_2 sensing at room temperature with the mobility (field-effect) of ~10^{-4} cm^2 V^{-1} s^{-1}. The sensitivity of the fabricated OFET device was extracted from the transistor characteristics (at Vgs = -30 V and Vds = -40 V) found to be ~4.8 × 10^{-3} nA/ppm. The device exhibited engrossing characteristics such as excellent recoverability (> 95%), with ultrafast response time (< 30 s) and greater sensitivity with high stability as can be assessed from the electrical characteristics.

Keywords: Bougainvillea, Poly(3-hexylthiophene), Zinc oxide nanoparticles, Nitrogen dioxide sensor.

INTRODUCTION

Due to unique structural and functional properties exhibited by nanostructured materials, these materials are trending research interests of the researchers owing to their extensive use in various fields of applications from the past two decades [1-3]. Considerably, the metal oxide nanostructured materials are most demanding in the field of sensor applications owing to their greater response, good selectivity and sensitivity [4-6]. Recently, the green-synthesis of these nanostructured materials has impacted their extensive use in various fields of applications due to their bio-compatibility, less-toxic and low-cost approach [7-9]. There has been always key prominence for green nanostructured materials owing to their control over material properties such as size; shape and morphology whereas the chemical and physical method based nanostructured materials are always strenuous. The green-synthesis majorly involves the use of plants, fruits, leaf extracts and biosynthesis involves use of microorganisms, bacteria, fungus as major source for synthesis of nanostructured materials [10-13]. Among these nanostructured metal oxide materials, zinc oxide (ZnO) and tin oxide (SnO_2) are most optimistic materials for field of sensors which may be attributed to physical, mechanical and biological sensing applications [14-17].

Zinc oxide is well-known for wide bandgap of 3.3-3.5 eV and large exciton energy (binding) of 60 meV, which can be synthesized with ease of synthesis process owing to the fact that ZnO is less-toxic, low-cost synthesis process and extensive use in healthcare and biomedical field due bio-compatibility nature [18-21]. It is an n-type semiconductor material with variety of structures (spherical, comb, flower, rods, cone, *etc.*) and has a great control over the size, shape and morphology

with much superior surface to volume ratio making room for variety of applications. Furthermore, the green-synthesized ZnO nanomaterial has certain notable chemical, physical, thermal and electrical properties, which reveal the prominence of the material to better suit in extensive applications. Besides, the ZnO nanostructured material in sensor application is known for its stability, selectivity and sensitivity as compared to other nanostructured metal oxides which are generally considered as the important aspects of sensor characteristics [22-27].

Herein, the green-synthesized nanostructured ZnO metal oxide particles as receptor (sensing) layer in the field effect transistor over the conducting polymer (poly-3-hexylthiophene) to detect NO_2 gas. The field effect transistors are extensive studied in the field of sensors owing to their fast, selective and sensitive response as compared to resistive and capacitive based sensors. The analysis of electrical parameters such as drain and transfer characteristics play major role in understanding the detection level of analytes exposed over the fabricated device. The other electrical parameters such as mobility (μ), drain saturation current (Idsat), ion-current (Ion) and off-current (Ioff) extracted from the drain and transfer characteristics of the device, which further confirms the sensors studies in terms of selectivity and sensitivity. In the present study, green-mediated ZnO nanoparticles synthesis using bougainvillea leaf extract arbitrated microwave assisted approach and the obtained nanoparticles were confirmed using various characterization techniques such as X-ray diffraction (XRD), scanning electron microscopy (SEM), energy dispersive X-ray analysis (EDAX) and UV-visible spectroscopy (UV-Vis). The fabricated field effect transistor device was electrically characterized using Keithley 4200-SCS source meter unit to understand the transfer and drain characteristics of the transistors for both cases of before and after exposure of NO_2 molecules. The aforesaid sensing performance of the device fabricated and the green-synthesized nanostructured material are also discussed.

EXPERIMENTAL

The LR grade zinc nitrate ($Zn(NO_3)_2{\cdot}6H_2O$) was procured from Thomas Baker, the requisite AR grade solvents such as isopropyl alcohol and ethanol were purchased from Merck whereas poly(3-hexylthiophene) (P3HT) was purchased from Sigma-Aldrich, USA.

Extraction of bougainvillea leaf: Fresh bougainvillea leaves were collected and cleaned under tap water followed by deionized water for 2-3 times to remove all sort of contaminations. These cleaned leaves of nearly 50 g weighed were shredded into pieces wearing gloves and rinsed in deionized water before the start of extraction process. The beaker with deionized water of 100 mL was stacked with those shredded leaf on magnetic stirrer with constant stirring of 400 rpm for 3 h at 120 ºC covering watch glass on top of the beaker partially. The change in the solution color from transparent to greenish indicated the formation of leaf extract which was then filtered using Whatman paper No. 1. The solution was further cooled at room temperature before considering it for synthesis process.

Synthesis of green-mediated ZnO nanoparticles: Aqueous solution of zinc nitrate was prepared by adding 0.3 M zinc nitrate in 60 mL of deionized water under room temperature stirring for 10 min which was further added into the as-prepared bougainvillea leaf extract of 60 mL (1:1 ratio). The resultant mixture was kept in microwave irradiation for 140 ºC for 30 min leading to the formation of precipitate collected at the bottom of beaker, which was centrifuged (for 5 min), washed and filtered (using Whatman filter paper grade 1) repeatedly using deionized water. The resultant product was transferred to silica crucible and dried in muffle furnace for 2 h at 120 ºC without any further delay to avoid native contaminations. The obtained nanoparticles were further grinded using agate mortar and stored for further charact-erization process to overview the material characteristics.

RESULTS AND DISCUSSION

X-ray diffraction studies: The crystallite size analysis was performed with Rigaku Ultima IV instrument and the pattern was recorded at room temperature in 2θ range of 200-800º along the crystallographic planes. The pattern depicted planes of (100), (002), (101), (012), (110), (103), (112), (201), (004), (202) and (113) for the values of 31.75º, 34.45º, 36.31º, 47.56º, 56.57º, 62.91º, 66.20º, 68.10º 69.23º, 72.37º and 77.22º, respectively (Fig. 1). The ZnO characteristic peaks associated along the crystallographic planes were in favorable with earlier published values and holds good with JCPDS card no. 80-0075. The hexagonal wurzite structure is elucidated by characteristic peaks corresponds to pure ZnO formation and no additional/uncharacteristic was seen, confirming the purity of green synthesized ZnO nanoparticles. The crystallite size of ZnO nanoparticles was revealed from the most intense peak considering the β (FWHM)) using Scherer formula: $D = k\lambda/\beta\cos\theta$; where, D = crystallite size, k = Scherer's constant (0.94), λ = diffraction wavelength, θ = diffraction angle. The average crystallite size (D) of as-synthesized ZnO nanoparticles was found to be 28 nm.

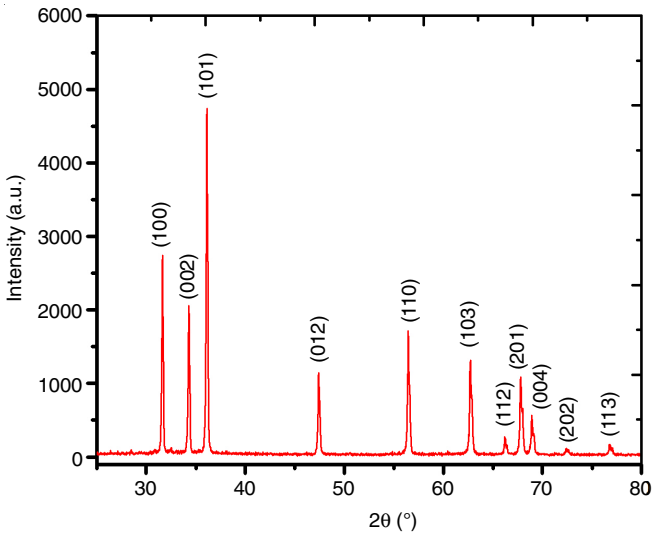

Fig. 1. XRD pattern recorded along intensity *vs.* 2θ (°) for bougainvillea leaf extract-mediated nanostructured ZnO nanoparticles

Morphological studies: The ZnO nanoparticles were dispersed in ethanol and sonicated prior to the drop-cast onto Si wafer for SEM and EDAX analysis. The MIRA3 TESCAN

instrument (SEM) was used to study the size/shape/surface morphology of the nanostructured ZnO material clearly evidencing the spherical shape aggregated and spread over few regions (Fig. 2a) and the cross-section of view ZnO nanoparticles drop-casted on to Si substrate (Fig. 2b). The average size distribution of nanostructured ZnO particles were in the range of ~ 20-50 nm as evidenced from Fig. 2a. The EDAX spectrum (Fig. 2c) illustrated the presence of Zn and O with small amount of organic moiety (carbon) as derived from the elemental composition of Zn with 71% and O with 24% (Fig. 2d) owing to the purity of the nanostructured material so obtained.

Optical absorption studies: The bougainvillea leaf extract mediated synthesis of nanostructured ZnO particles were further subjected to absorption studies using UV-visible spectrometer LAMBDA 750 and absorbance vs wavelength was plotted (Fig. 3a) and a plot of $(\alpha h\nu)^2$ *versus* $h\nu$ was exploited from the Tauc relation to study the optical bandgap (Eg) from the linear plot was found to be 3.6 eV (inset Fig. 3a). The optical absorption was recorded for the wavelength range of 200-650 nm by dispersing the ZnO nanoparticles (green/biogenic synthesized) in ethanol (orthogonal solvent) and exposing the solution under UV light. A high retention coefficient in the UV region was uncovered by the spectra of ZnO, whereas in the visible range found transparent. The absorption aroused at 374 nm corresponds to 3.6 eV with increased carrier concentration as estimated from the optical absorption measurements. Similarly, the intensity *versus* wavelength plot was recorded for photophysical property studies as can be seen from Fig. 3b. The sturdy peaks aroused at 410 and 433 nm can be attributed to strong blue emission with intrinsic defects of different species and peak at 458 nm can be ascribed to the transition of electrons from interstitial Zn to valence band (top) and conduction band transition to oxygen defect [28,29].

Transistor device fabrication process: The transistor device was fabricated by considering the substrate as Si wafer (2-inch), polished (single-sided) with low resistivity of 0.01-0.02 Ω cm (n-type) prior coated with dielectric layer (SiO_2) thickness of ~140 nm. The substrate was cleaned (ultrasonically) using acetone and isopropyl alcohol (IPA) wash followed by deionized water repeatedly to remove any sort of contaminations. The green/biogenic synthesized ZnO nanoparticles were dispersed in ethanol and the P3HT solution (1 mg in 2 mL

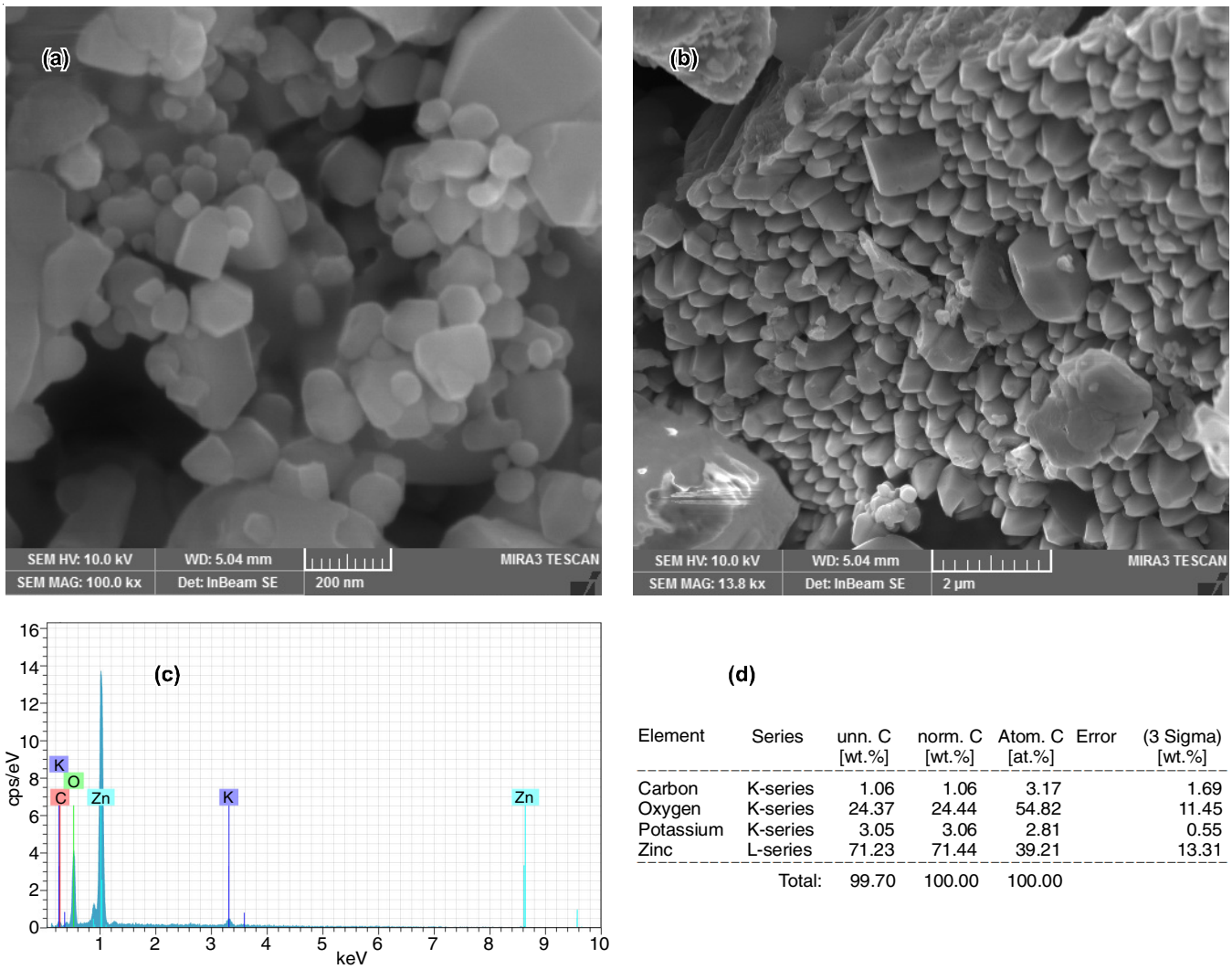

(d)

Element	Series	unn. C [wt.%]	norm. C [wt.%]	Atom. C [at.%]	Error	(3 Sigma) [wt.%]
Carbon	K-series	1.06	1.06	3.17		1.69
Oxygen	K-series	24.37	24.44	54.82		11.45
Potassium	K-series	3.05	3.06	2.81		0.55
Zinc	L-series	71.23	71.44	39.21		13.31
	Total:	99.70	100.00	100.00		

Fig. 2. SEM image of bougainvillea leaf extract-mediated ZnO nanoparticles: (a) with magnification of 200 nm; (b) the cross-section view at 2 µm and (c) EDAX spectrum confirming the elemental composition; (d) stoichiometric analysis of ZnO nanoparticles

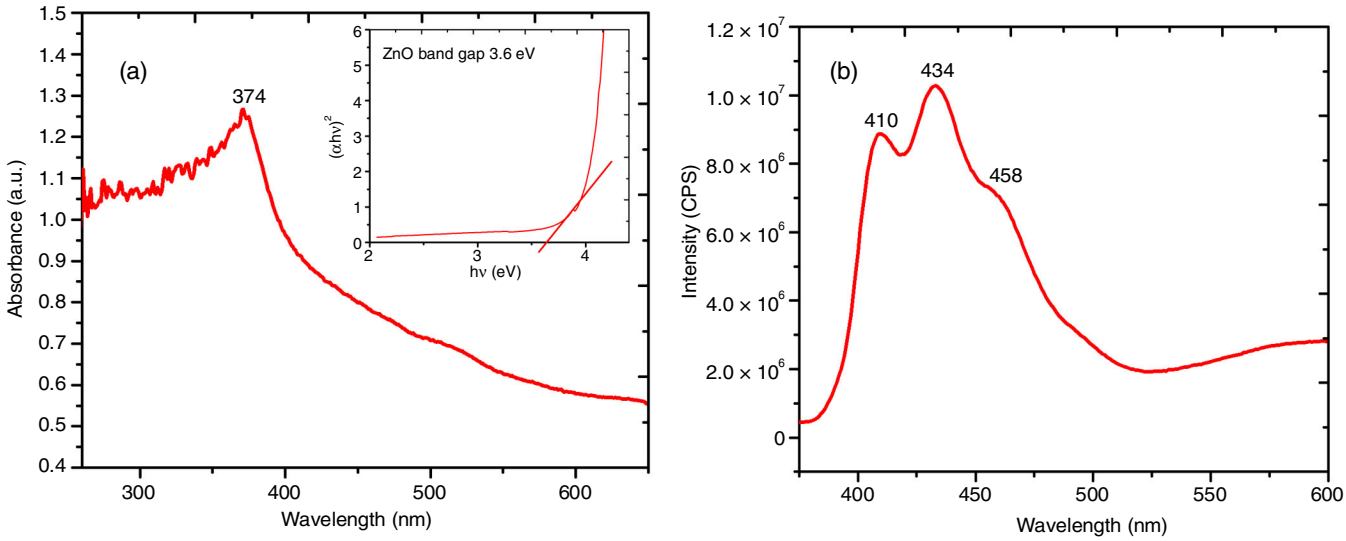

Fig. 3. Photoluminescence spectra recorded for green synthesized ZnO nanoparticles: (a) UV absorption spectra of absorbance *vs.* wavelength (200-650 nm) and bandgap plot using Tauc relation (inset Fig. 4b); (b) intensity *vs.* wavelength range of 200-600 nm

of 1,2-dichlorobenzene) was spun with rotation speed of 1500 rpm for 30 s, while the ZnO solution was spun for 45 s at 1200 rpm under argon atmosphere inside the glove-box. The resultant substrate was annealed at 120 ºC for 90 min prior to the deposition (sputtered using physical mask) of contact pads (Au) for drain and source terminals (~60 nm) [30]. The fabricated transistor device is further characterized using Keithley 4200-SCS for the analysis of transistor behavior for before and after exposure of NO_2 molecules as shown in Fig. 4.

Sensor characteristics analysis: The fabricated transistor devices were electrically characterized to understand the transistor behaviour by recording the transfer (input) and drain (output) characteristics using source meter. The transfer characteristics of p-type device was recorded by applying the voltage across gate terminal 0 to -36 V (with interval of -1 V), while the voltage across drain terminal was maintained constant (-10 to -30 V with -5 V as interval) for which the current across drain terminal is recorded (Fig. 5a). Similarly, the drain character-

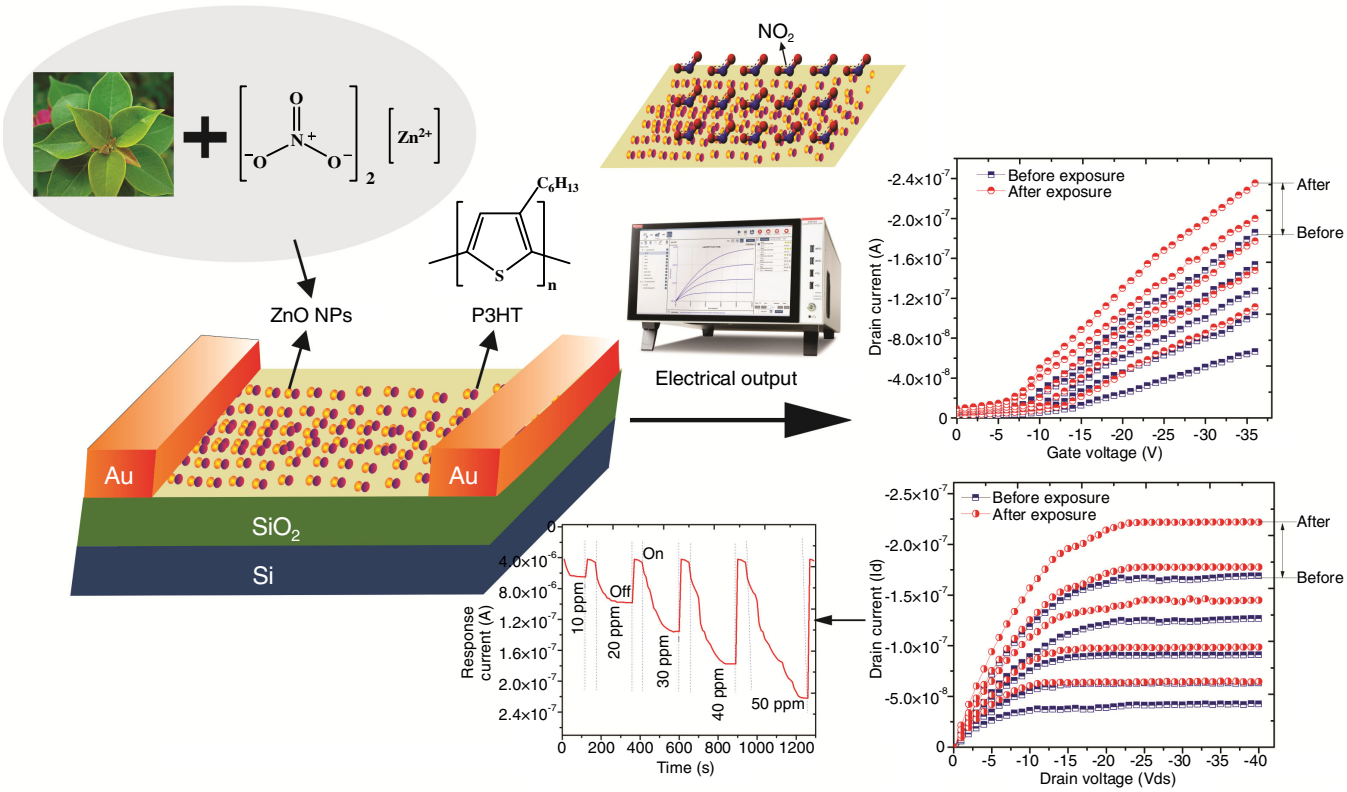

Fig. 4. Transistor device fabricated for sensing NO_2 molecules using P3HT (conduction channel) and ZnO (receptor layer) and the schematic representation highlights the transfer and drain characteristics for before and after the exposure of NO_2 molecules and response graph recorded

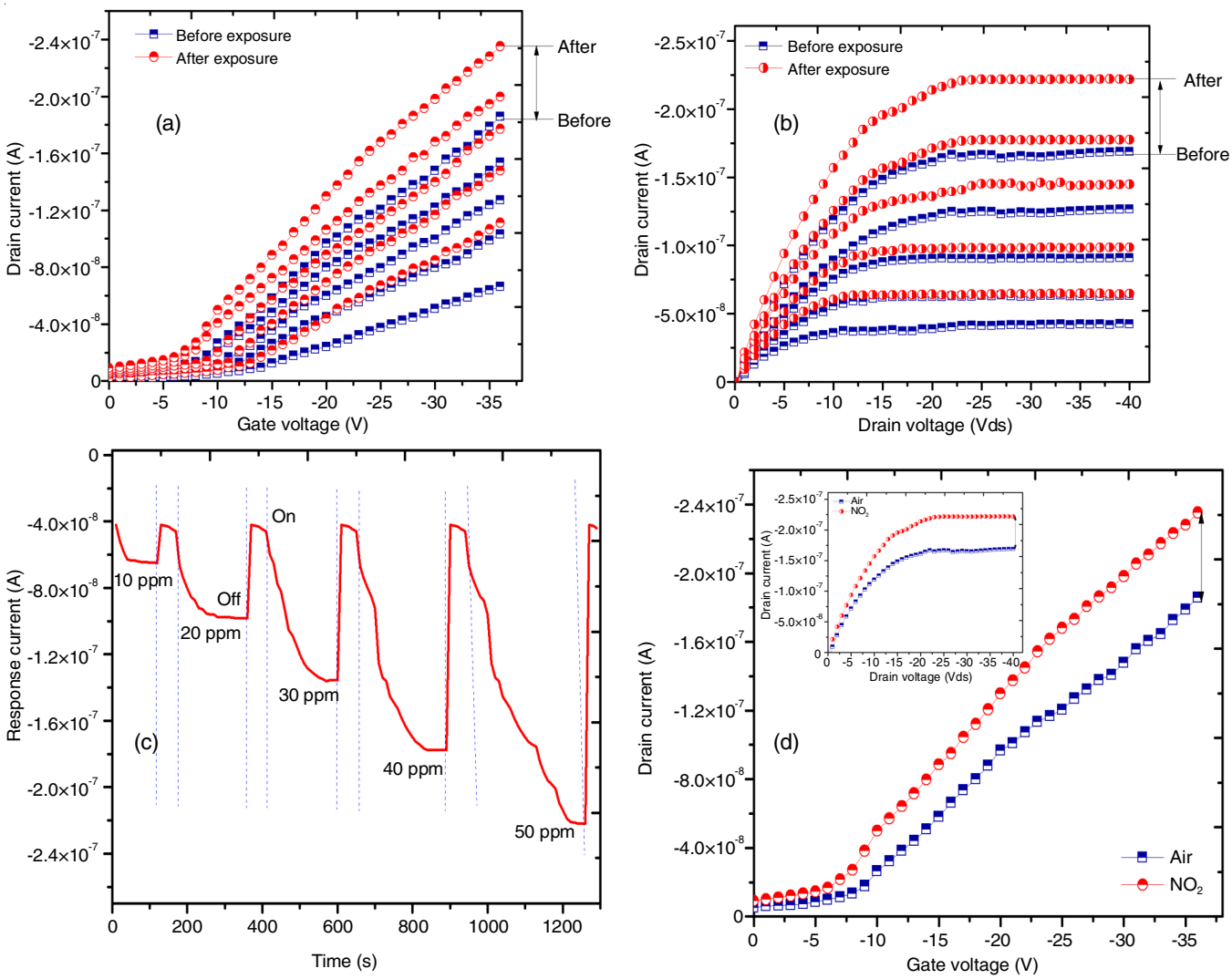

Fig. 5. OFET device electrical characteristics: (a) transfer; (b) drain; (c) response curve plot for NO_2 sensing at different concentrations (d) transfer characteristics at Vds = -30 V and Vgs = -36 V and drain characteristics at Vds = -40 V and Vgs = -30 V (inset) with and without exposure

istics was recorded by varying the voltage across drain terminal from 0 to -40 V (interval of -1 V) maintaining the constant voltage across gate terminal for different values from -10 to -30 V with interval of -5 V as can be seen from Fig. 5b. The input and output characteristics recorded for before and after exposure of NO_2 molecules clearly evidenced the molecular interaction of NO_2 with ZnO. They tend to have always a strong interaction owing to the fact that Zn gets partially oxidized and nitrated forming a combination result [31]. The adsorption of sub-atomic and nuclear oxygen on the outside of ZnO nanoparticles makes an electron-exhausted space-charge layer, a significant attribute of the receptor work. This adsorbed oxygen further decides the surface charge layer thickness, surface potential obstruction stature and surface charge. The NO_2 gas on the outside of the ZnO nanoparticles gets diminished by the exchange of the electrons from the conduction band, along these lines expanding the electron-drained layer and thus bringing about more extensive intersection potential boundaries This builds the obstruction of ZnO layer with broadening of the intersection expected hindrances, thereby confirming the sensing ability of ZnO layer towards the NO_2 molecules [32-35]. The increase in the drain and transfer characteristics after the NO_2 is due to P3HT layer lesser the charge carrier interaction with ZnO molecules reduces the resistance effect, thus increases the current flow in due course of ZnO interaction with NO_2. The response current *versus* time plot (Fig. 5c) for various concentration of NO_2 evidences the excellent recoverability (> 95%), with ultra-fast response time (< 30 s) and greater sensitivity and stability as per test results can be ascribed.

The sensing measurements were carried out at room temperature and the NO_2 exposure (0 to 50 ppm) considered was well-under Occupational Safety and Health Administration (OSHA) standards. The transistor behaviour for gas sensing was recorded for transfer characteristics at Vds = -30 V and Vgs = -36 V and drain characteristics at Vds = -40 V and Vgs = -30 V (inset Fig. 5d) clearly evidences that the transient response shows clear analysis over sensing ability of the fabricated P3HT/ZnO based transistor device as can be seen from Fig. 5d. The mobility (field-effect) of the fabricated OFET device was found to be 10^{-4} cm^2 V^{-1} s^{-1} and the sensitivity extra-

cted from the transistor characteristics (at Vgs = -30 V and Vds = -40 V) was found to be 4.8 × 10^{-3} nA/ppm.

Conclusion

In this work, a green-mediated synthesis of zinc oxide nanoparticles using microwave assisted approach and the incorporation of these ZnO nanoparticles (as receptor layer) in OFET devices for NO_2 sensing was carried out. The as-synthesized ZnO nanoparticles chemical and photophysical properties were also determined. The XRD revealed the crystallite structure (hexagonal wurzite) while the SEM confirmed the particle size in the range of ~ 20-50 nm. The fabricated OFET device using P3HT/ZnO nanoparticles was electrically characterized for before and after exposure of NO_2 molecules (0 to 50 ppm) confirmed the sensing ability of the device. The mobility (field-effect) of the fabricated OFET device showed ~ 10^{-4} cm^2 V^{-1} s^{-1} and the sensitivity extracted from the transistor characteristics (at Vgs = -30 V and Vds = -40 V) was ~ 4.8 × 10^{-3} nA/ppm. The device exhibited engrossing characteristics such as excellent recoverability (> 95%), with ultrafast response time (< 30 s) and greater sensitivity with high stability. Thus, the fabricated sensor device can be promising near future of nano e-devices with excellent performances in real time applications.

CONFLICT OF INTEREST

The authors declare that there is no conflict of interests regarding the publication of this article.

REFERENCES

1. J. Jeevanandam, A. Barhoum, Y.S. Chan, A. Dufresne and M.K. Danquah, *Beilstein J. Nanotechnol.*, **9**, 1050 (2018); https://doi.org/10.3762/bjnano.9.98
2. A. Rani, R. Reddy, U. Sharma, P. Mukherjee, P. Mishra, A. Kuila, L.C. Sim and P. Saravanan, *J. Nanostruct. Chem.*, **8**, 255 (2018); https://doi.org/10.1007/s40097-018-0278-1
3. A. Gentile, F. Ruffino and M. Grimaldi, *Nanomaterials*, **6**, 110 (2016); https://doi.org/10.3390/nano6060110
4. L. Chacko, E. Massera and P.M. Aneesh, *J. Electrochem. Soc.*, **167**, 106506 (2020); https://doi.org/10.1149/1945-7111/ab992c
5. K. Xu, C. Fu, Z. Gao, F. Wei, Y. Ying, C. Xu and G. Fu, *Instrum. Sci. Technol.*, **46**, 115 (2018); https://doi.org/10.1080/10739149.2017.1340896
6. D. Nunes, A. Pimentel, A. Gonçalves, S. Pereira, R. Branquinho, P. Barquinha, E. Fortunato and R. Martins, *Semicond. Sci. Technol.*, **34** 043001 (2019); https://doi.org/10.1088/1361-6641/ab011e
7. R. Mohammadinejad, S. Karimi, S. Iravani and R.S. Varma, *Green Chem.*, **18**, 20 (2016); https://doi.org/10.1039/C5GC01403D
8. R.K. Mishra, S.K. Ha, K. Verma and S.K. Tiwari, *Adv. Mater. Devices*, **3**, 263 (2018); https://doi.org/10.1016/j.jsamd.2018.05.003
9. M. Jeyaraj, S. Gurunathan, M. Qasim, M.H. Kang and J.H. Kim, *Nanomaterials*, **9**, 1719 (2019); https://doi.org/10.3390/nano9121719
10. P. Khandel, R.K. Yadaw, D.K. Soni, L. Kanwar and S.K. Shahi, *J. Nanostruct. Chem.*, **8**, 217 (2018); https://doi.org/10.1007/s40097-018-0267-4
11. P. Khandel and S.K. Shahi, *J. Nanostruct. Chem.*, **8**, 369 (2018); https://doi.org/10.1007/s40097-018-0285-2
12. M. Ovais, A. Khalil, M. Ayaz, I. Ahmad, S. Nethi and S. Mukherjee, *Int. J. Mol. Sci.*, **19**, 4100 (2018); https://doi.org/10.3390/ijms19124100
13. X. Li, H. Xu, Z.S. Chen and G. Chen, *J. Nanomater.*, **2011**, 270974 (2011); https://doi.org/10.1155/2011/270974
14. A.I. Ayesh, *J. Nanomater.*, **2016**, 1 (2016); https://doi.org/10.1155/2016/2359019
15. N. Tripathy and D. Kim, *Nano Converg.*, **5**, 27 (2018); https://doi.org/10.1186/s40580-018-0159-9
16. S. Sudhaparimala and M. Vaishnavi, *Mater. Today Proc.*, **3**, 2373 (2016); https://doi.org/10.1016/j.matpr.2016.04.150
17. H. Du, X. Li, P. Yao, J. Wang, Y. Sun and L. Dong, *Nanomaterials*, **8**, 509 (2018); https://doi.org/10.3390/nano8070509
18. A. Narayana, S.A. Bhat, A. Fathima, S.V. Lokesh, S.G. Surya and C.V. Yelamaggad, *RSC Adv.*, **10**, 13532 (2020); https://doi.org/10.1039/D0RA00478B
19. V.N. Kalpana and V.D. Rajeswari, *Bioinorg. Chem. Appl.*, **2018**, 3569758 (2018); https://doi.org/10.1155/2018/3569758
20. W. Muhammad, N. Ullah, M. Haroon and B.H. Abbasi, *RSC Adv.*, **9**, 29541 (2019); https://doi.org/10.1039/C9RA04424H
21. M. Shaban, F. Mohamed and S. Abdallah, *Sci. Rep.*, **8**, 3925 (2018); https://doi.org/10.1038/s41598-018-22324-7
22. R. Kumar, O. Al-Dossary, G. Kumar and A. Umar, *Nano-Micro Lett.*, **7**, 97 (2015); https://doi.org/10.1007/s40820-014-0023-3
23. H. Beitollahi, S. Tajik, F. Garkani Nejad and M. Safaei, *J. Mater. Chem. B Mater. Biol. Med.*, **8**, 5826 (2020); https://doi.org/10.1039/D0TB00569J
24. G.H. Mhlongo, D.E. Motaung, F.R. Cummings, H.C. Swart and S.S. Ray, *Sci. Rep.*, **9**, 9881 (2019); https://doi.org/10.1038/s41598-019-46247-z
25. S. Chaudhary, A. Umar, K. Bhasin and S. Baskoutas, *Materials*, **11**, 287 (2018); https://doi.org/10.3390/ma11020287
26. Y. Zhang, M.K. Ram, E.K. Stefanakos and D.Y. Goswami, *J. Nanomater.*, **2012**, 624520 (2012); https://doi.org/10.1155/2012/624520
27. M.M. Rahman, H.B. Balkhoyor and A.M. Asiri, *RSC Adv.*, **6**, 29342 (2016); https://doi.org/10.1039/C6RA02352E
28. J. Kegel, F. Laffir, I.M. Povey and M.E. Pemble, *Phys. Chem. Chem. Phys.*, **19**, 12255 (2017); https://doi.org/10.1039/C7CP01606A
29. H. Chen, J. Ding, W. Guo, G. Chen and S. Ma, *RSC Adv.*, **3**, 12327 (2013); https://doi.org/10.1039/c3ra40750k
30. A. Narayana, S.U. Kumar, N. Tarannum and S.V. Lokesh, *Sens. Lett.*, **17**, 581 (2019); https://doi.org/10.1166/sl.2019.4113
31. J.A. Rodriguez, T. Jirsak, J. Dvorak, S. Sambasivan and D. Fischer, *J. Phys. Chem. B*, **104**, 319 (2000); https://doi.org/10.1021/jp993224g
32. M.J.S. Spencer and I. Yarovsky, *J. Phys. Chem. C*, **114**, 10881 (2010); https://doi.org/10.1021/jp1016938
33. R.K. Sonker, B.C. Yadav, A. Sharma, M. Tomar and V. Gupta, *RSC Adv.*, **6**, 56149 (2016); https://doi.org/10.1039/C6RA07103A
34. M.A. Chougule, S.R. Nalage, S. Sen and V.B. Patil, *J. Exp. Nanosci.*, **9**, 482 (2014); https://doi.org/10.1080/17458080.2012.670275
35. S. Han, J. Cheng, H. Fan, J. Yu and L. Li, *Sensors*, **16**, 1763 (2016); https://doi.org/10.3390/s16101763